# Control of electrical turbulence by periodic excitation of cardiac tissue

Pavel Buran,[1] Markus Bär,[1] Sergio Alonso,[2] and Thomas Niedermayer[1, a)]
[1)] *Physikalisch-Technische Bundesanstalt (PTB), Abbestr. 2–12, 10587 Berlin, Germany*
[2)] *Department of Physics, Universitat Politècnica de Catalunya, Av. Dr. Marañón 44, 08028 Barcelona, Spain*

(Dated: 30 June 2017)

Electrical turbulence in cardiac tissue is associated with arrhythmias such as the life-threatening ventricular fibrillation. The application of a high-energy electrical shock constitutes an effective defibrillation, but also causes severe side effects. Recent experimental studies have shown that a sequence of low energy electrical far-field pulses is able to terminate fibrillation more gently than a single pulse. During this low-energy antifibrillation pacing (LEAP) only tissue near sufficiently large conduction heterogeneities, such as large coronary arteries, is activated. In order to understand and potentially optimize LEAP, we performed extensive simulations of cardiac tissue perforated by blood vessels. We checked three alternative cellular models that exhibit qualitatively different electrical turbulence. LEAP may operate if and only if the spectrum of this chaotic activity is characterized by a narrow peak around a dominant frequency. For each of 100 initial conditions, we tested different electrical field strengths, pulse shapes, numbers of pulses, and periods between the pulses. It turned out that the optimal period matches the dominant period of the chaotic activity while both over- and underdrive pacing lead to a considerably smaller success probability and higher field strength for reliable defibrillation. An optimal LEAP protocol, which minimizes the required total energy for successful defibrillation, consists of five or six pulses. Compared to a single bi-phasic defibrillation pulse, it reduces the total energy by about 86%, corresponding to an energy reduction of 97 – 98% per pulse.

PACS numbers: ...
Keywords: cardiac modeling, excitable media, defibrillation, low-energy antifibrillation pacing (LEAP)

**In ventricular fibrillation, the heart is quivering instead of pumping, a condition which leads to cardiac arrest and ultimately to death. This loss of synchronous contraction stems from disorganized electrical activity in the ventricles. Emergency defibrillation is achieved by the application of a strong electrical shock which is accompanied by severe side effects such as tissue damage and trauma. Recently, an alternative treatment using a sequence of low energy pulses has been suggested in which each electrical pulse excites only localized tissue sites at the large heterogeneities – such as blood vessels – instead of the entire tissue. In laboratory experiments in vitro and in vivo, this so-called low-energy antifibrillation pacing (LEAP) with five pulses achieves defibrillation with an energy reduction of 80 – 90 % per pulse in comparison with standard single shock treatment. Here, we perform an extensive numerical study of LEAP employing far field pacing at the major blood vessels. We have tested three alternative electrophysiological models that exhibit qualitatively different spatiotemporally chaotic activity. LEAP operates if and only if the spectrum of this chaotic activity is characterized by a narrow peak around a dominant frequency. In this case, a resonant pacing with the same frequency and a sequence of five to six pulses results in an optimal total energy reduction for defibrillation of 86 % and an even greater reduction per pulse. Pacing with a frequency which is similar, but somewhat different from the dominant frequency, as typically done in experiments, results in a considerably smaller energy reduction. Our results may provide a link between the spectrum of the electrical activity and the optimal pacing frequency in experimental defibrillation procedures.**

## I. INTRODUCTION

A loss of rhythm and synchronization of cardiac electrical impulses orchestrating the pumping of blood is associated with a number of arrhythmias (i.e. abnormal or irregular heart rhythms) including atrial fibrillation (AF), ventricular fibrillation (VF), and ventricular tachycardia (VT). The nonlinear dynamics of electrical excitation waves in cardiac tissue has been studied extensively in experiment and simulation for more than two decades, for recent reviews see e. g.[1–5]. VF represents a particularly dangerous malfunction of the heart, in which synchronous excitation and contraction of different parts of the ventricles is lost, potentially causing sudden death if left untreated for more than a few minutes.

The electrical activity during VF is dominated by either one or a few large rotors (mother rotors) surrounded by irregular activity or entirely by multiple wavelets in a spatiotemporally chaotic state. First direct experimental

[a)] Electronic mail: niedermayerthomas@gmail.com

observations of such states were reported almost 20 years ago[6,7]. Recent experimental and simulations studies[8,9] show a complex picture with states dominated by one or a few mother rotors as well as multiple wave dynamics characterized by a mean number of 10 vortices on the surface of, e. g., a human heart. The fluctuations in vortex number resemble a Poissonian statistics.

Defibrillation by a strong electrical pulse is the only known effective therapy for VF. Such a strong shock globally excites the tissue resulting in termination of all excitation waves, but also causes severe side effects as pain and trauma for the patient[10], damage of the myocardium[11], and reduced battery life in implanted devices. These adverse effects could be diminished if VF could be terminated reliably by defibrillation shocks with significantly lower energies. Recent studies[12,13] of AF in vitro and in vivo as well as VF in vitro have shown that a sequence of five low-energy far-field pulses with stimulation rates close to the arrhythmia cycle length can require $80-90\%$ less energy per pulse than a single shock. This method is called low-energy antifibrillation pacing (LEAP). With much faster pacing rates than the cycle length, similar energy reductions were found for AF[15,16], while for VT the energy may further be reduced by an order of magnitude[14,17].

LEAP takes advantage of the fact that an electric field depolarizes and hyperpolarizes the tissue near conductivity heterogeneities[18] which become virtual electrodes[19]. The strength of this effect depends on the size and shape of the heterogeneities and the strength of the electric field[20–22]. Only tissue at major conduction heterogeneities may be activated by each of these very weak pulses. Therefore, global tissue activation and wave termination originates from few localized activation sites (hot spots). The mechanism how multiple low-energy far-field pulses terminate arrhythmias are not well understood as experimental methods to visualize three dimensional electrical turbulence are missing. Luther et al.[13] suggest that the major conduction heterogeneities necessary for LEAP are given by large coronary arteries and show that the size distribution of the heterogeneities follows a power law. However, Caldwell et al.[23] did not find such a co-localization of hot spots and major coronary vessels.

Theoretical approaches to understand LEAP have often focussed on the process of unpinning and removal of a small number of vortices[20,24–26]. In these papers, it was demonstrated that vortices that were assumed to be pinned at larger heterogeneities in cardiac tissue are best terminated if the pacing frequency in a LEAP procedure is set to be 80 - 90% of the dominant frequency (the rotation frequency of the vortex around the pinning site). Such a choice of pacing frequency allows for an efficient scanning of the phase of the vortex in order to find the vulnerable window for vortex termination[27,28]. A simulation study in a realistic three-dimensional cardiac geometry demonstrated for selected examples that LEAP works for a pacing period of 88% of the VF cycle length, but often fails for much faster pacing with a period of 16% of the VF cycle length[29].

For LEAP, reduction of defibrillation energy is the quantity which is studied in the quasi-two-dimensional AF and the three dimensional VF[13]. Very similar results are found in both cases and, moreover, the size distribution of the radii of arteries are found to be almost identical for atria and ventricles. Therefore, we expect that LEAP can be qualitatively investigated within a simple two dimensional model in which the non-conducting heterogeneities are represented by circles whose size distribution is given by the distribution of radii of coronary arteries measured in[13]. Furthermore, we employed three alternative models which are established for ventricular cells[32–34]. The simplicity of our composite model allows us to perform systematic statistical studies with a set of 100 initial conditions. This is essential since both standard defibrillation and LEAP may depend critically on these and are also associated with large uncertainties[13].

In our computational study, we aim for a basic understanding of LEAP to potentially optimize its protocol. Therefore, we have investigated many aspects of LEAP which might be crucial for its success. It turns out that for successful LEAP, both the electrical turbulence and the LEAP protocol must posses certain properties. Moreover, we found a LEAP protocol which is even more efficient in our simulations than the one employed in experimental studies.

In the methods section 2, we introduce the cellular models in a mono-domain framework, the distribution of heterogeneities, the alternative defibrillation protocols, the numerical methods used in the simulations, and our choice of initial conditions. Section 3 contains the main results regarding characterization of electrical turbulence in the three models, single pulse defibrillation and LEAP as well as the survival statistics of fibrillation activity in the absence of defibrillation. Section 4 and 5 provide a discussion of the result and a short conclusion, respectively.

## II. METHODS

We have performed extensive numerical simulations with several cellular models and defibrillation protocols with different electrical field strengths, wave forms, number of pulses, and inter-pulse intervals. Typically, 100 simulation runs with different initial conditions were performed for each configuration. To obtain statistically valid results, we restricted the simulations to a homogeneous, isotropic and two-dimensional tissue which is perforated by blood vessels.

### A. Mono-domain equation and cellular models

By homogenization, cardiac tissue is represented by intra-cellular and extra-cellular space[5,30]. Assuming van-

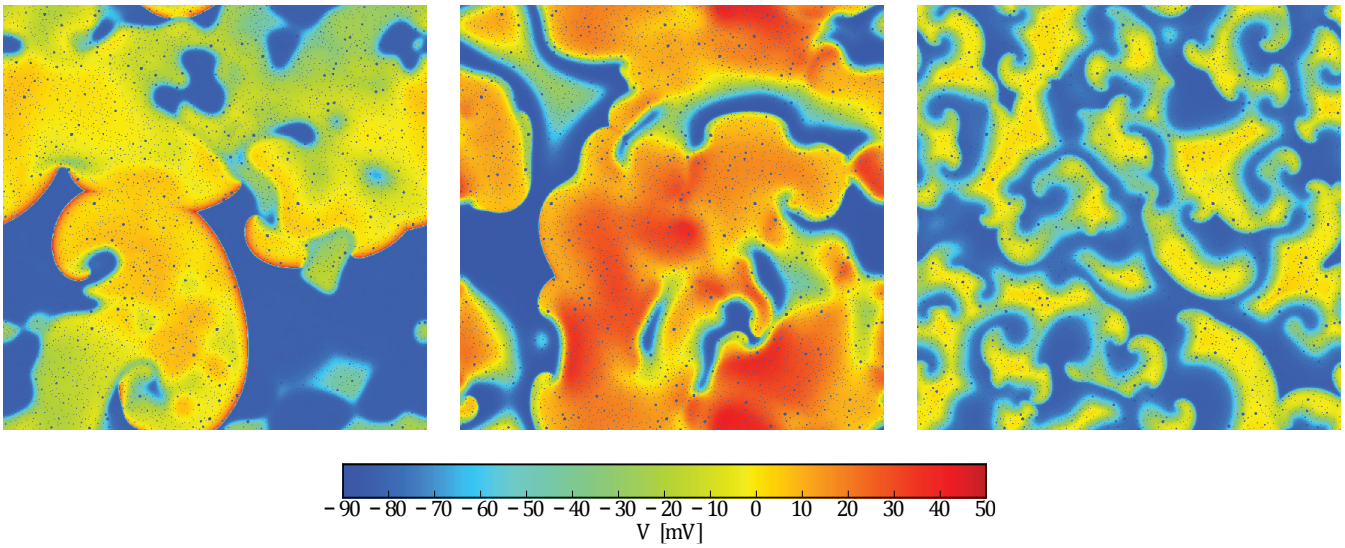


FIG. 1. (Color online) Snapshots of the transmembrane potential $V$ during electrical turbulence for the (LR, left), (TT, middle), and (FK, right) model with periodic boundary conditions. Movies of the simulations are provided as supplementary material. Simulations were performed on a rectangular domain with an edge length of 20 cm. The conductivity heterogeneities appear as small blue circles.

ishing anisotropy, the propagation of electrical waves is described by the mono-domain equation[30]:

$$\partial_t V(\vec{x},t) = D\,\Delta V(\vec{x},t) - \frac{I_{\text{ion}}\left(V(\vec{x},t),\vec{w}(\vec{x},t)\right)}{C}, \quad (1)$$

where $V$ denotes the transmembrane potential, $\Delta$ the Laplacian, $C$ the specific membrane capacitance, and $I_{\text{ion}}$ the sum of transmembrane current densities which is a function of both the transmembrane potential $V$ and several state variables $\vec{w}$. The (diffusion) coefficient $D$ is determined by tissue conductivity, membrane capacitance, and the area to volume ratio of the cellular model.

The dynamics of the state variables $\vec{w}$ in eq. (1) is specified by a particular cellular model. To our knowledge, reliable information about the structure of electrical turbulence during ventricular fibrillation is lacking, as cellular models are built to reproduce the activity in single cells and even recent models of human ventricular cells exhibit a very diverse spatiotemporal behavior[31]. Thus, we tested several cellular models which exhibit qualitatively different spatiotemporal chaos: The Luo-Rudy (LR) model with standard parameter values[32], the Ten Tusscher (TT) model with parameter values to match human epicardial tissue[33], and the Fenton-Karma (FK) model[34]. For the latter model, we have used the default parameter values in[35] which maximize the propensity for spiral waves to break while minimizing core meandering. In all three models we used the specific capacitance for cells of a mammalian heart, given by $C = 1.0\,\mu\text{F cm}^{-2}$ [36].

### B. Blood vessels as heterogeneities

Blood vessels constitute large heterogeneities of conductivity[13] and were modeled as non-conducting patches in otherwise homogenous tissue. The intracellular current into these heterogeneities is zero and in the presence of an external electric field $\vec{E}$, this leads to the boundary condition $(\nabla V - \vec{E}) \cdot \vec{n} = 0$[20,22], where $\vec{n}$ is normal to the boundary of the heterogeneity. In consequence, an external electric field, increases the transmembrane potential in the vicinity of one side of the heterogeneity and may activate this tissue[20,22]. In general, smaller heterogeneities require a larger field strength for tissue activation[20]. For a circular heterogeneity in quiescent two-dimensional tissue, the minimal radius required for activation is a well-known, monotonically decreasing function of the magnitude of the applied field[13,20]. In the absence of conduction heterogeneities and tissue anisotropy, the transmembrane potential is not altered by an external electrical field[30].

Both in ventricles and in atria of adult beagle dogs, the size distribution of coronary artery radii $R$ is given by a power law $p(R) \propto R^{\alpha}$[13]. This distribution holds between $R_{\text{min}} \approx 0.06\,\text{mm}$ and $R_{\text{max}} \approx 0.8\,\text{mm}$ and the exponent is given by $\alpha \approx -2.75$ both for ventricles and atria[13]. We modeled coronary arteries in ventricles as circular heterogeneities with radii drawn from this distribution and positions drawn from an uniform distribution while circle overlap is prohibited. For the (area) density of all heterogeneities, $40/\text{cm}^2$ was chosen since this value matches the measured density of activated arteries in the limit of large $E$[13]. We have checked that different realization of positions and radii resulted in almost identical

defibrillation successes. Therefore, the same realization of positions and radii was used in simulations while the initial states of electrical turbulence were varied unless stated otherwise.

### C. Defibrillation protocols

State-of-the-art defibrillators execute a biphasic, asymmetric protocol[37]. We tested both monophasic and biphasic defibrillation protocols specified as follows. For monophasic pulses, a rectangular waveform with a duration of 10 ms and amplitude $E$ was chosen. For biphasic pulses, the waveform consisted of two subsequent rectangular parts with identical amplitudes $E$ and opposite field direction. We fixed the total pulse duration to 10 ms and optimized the ratio of forward to backward duration. For fixed parameters, we found that 7 ms (forward) and 3 ms (backward) leads to best defibrillation results, in agreement with[38,39], where the best efficiency is obtained when the first phase is about twice as long as the second phase. Our low-energy antifibrillation pacing (LEAP) protocol contains $n$ identical biphasic pulses, where the interval $T$ between two pulses is constant and defined between the onsets of neighboring pulses.

### D. Numerical methods

The mono-domain eq. (1) in conjunction with a cellular model (LR, TT, or FK) was solved on an rectangular, 2-dimensional, and equidistant finite-difference grid with $1000\times1000$ nodes and a grid spacing of 0.2 mm, corresponding to an edge length of 20 cm. Both periodic and no-flux boundary conditions were used, as discussed below. The diffusion term of eq. (1) was discretized by the standard five-point stencil[40]. Since a straightforward explicit Euler time integration requires a rather small time step of 0.001 ms for numerical stability, we used the Rush-Larsen method[41] to integrate the gating variables. Furthermore, we considered the diffusion term implicitly, since for the explicit solution, time steps would have been limited by $\Delta x^2/4D$.[42] The resulting linear equation system has a symmetric positive definite coefficient matrix and can be solved efficiently by the conjugate gradient method[40]. These modifications allowed us to increase the time step to 0.1 ms.

### E. Generation of initial conditions

A single spiral wave was initiated using the standard cross-field stimulation technique[43] on a grid with no-flux boundary conditions. We have run the system for 5 s to allow spiral break and onset of electrical turbulence. Subsequently, the transmembrane potential in 10 randomly chosen squares with 10 mm edge length was set to the excitation threshold, the boundary conditions were changed (periodic or no-flux, depending on the simulations performed later), and the systems evolved for one more second to establish different initial conditions. In total, we generated 100 initial states of electrical turbulence (fibrillation) which we used for simulations with (LR), (TT), and (FK) cellular models, both with periodic and no-flux boundary conditions.

## III. RESULTS

### A. Electrical turbulence

After generating the initial conditions as discussed above, all considered cellular models – (LR), (TT), and (FK) – support electrical turbulence representing fibrillation, see fig. 1 and movies as supplementary material. However, the spectra of the transmembrane potential are qualitatively different: The (LR) model exhibits a pronounced peak indicating a dominant cycle length of $\tau = 1/f \approx 0.33$ s while the main peaks in the spectra of the (TT) and the (FK) model are more expanded, see fig. 2. Moreover, the (LR) spectrum features two additional peaks at about half and double of the dominant cycle length while the (TT) and (FK) spectra are rather unstructured.

Previous simulation studies have indicated that spatiotemporal chaos in generic one- and two-dimensional reaction-diffusion systems[44–46] and electrical turbulence in cardiac tissue[35] are often transient states. Therefore, we have checked the lifetimes of electrical turbulence in the absence of defibrillation and with initial conditions generated as described in section II E. With no-flux boundaries, both the (LR) and the (TT) model exhibit rather short spatiotemporal chaos while the turbulence in the (FK) model is quite persistent, see fig. 3. Naturally, periodic boundaries increase turbulence lifetimes and we find $t_{1/2} \approx 9.2$ s for the half-life of the turbulence in the (LR) model. The half-lifes of both the other models are beyond our simulation horizon.

### B. Single pulse defibrillation

Running $N = 100$ simulations (see supplementary material) for each parameter configuration and starting from different initial conditions as presented above, we determined the single pulse termination probability $P^{\mathrm{S}}$, which is defined as the probability that a fibrillation state is converted into a quiescent state by a single defibrillation pulse, as a function of field strength $E$. We computed $P^{\mathrm{S}}$ as the fraction of successful termination events, see fig. 4. This is a statistically sound estimate since its error is given by $\delta P^{\mathrm{S}} = \sqrt{P^{\mathrm{S}}(1-P^{\mathrm{S}})/N} \sim 1/\sqrt{N}$. We have checked both mono-phasic and bi-phasic pulse protocols as well as both periodic and no-flux boundary conditions. For a given cellular model and fixed pulse duration, bi-phasic pulses (3 ms forward, 7 ms backward) are

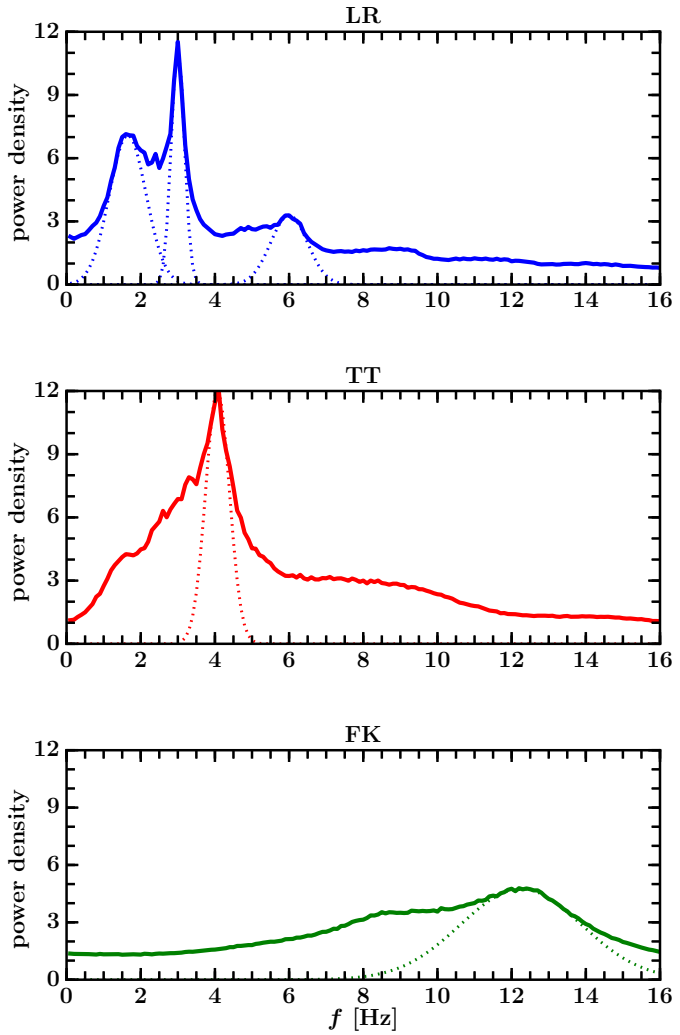


FIG. 2. (Color online) Spectra of transmembrane potential $V$ during electrical turbulence for the Luo-Rudy[32] (LR, top), Ten Tusscher[33] (TT, middle), and Fenton-Karma[34] (FK, bottom) model. Simulations were performed for 10 s and with 10 different initial conditions exhibiting electrical turbulence. The displayed graphs are averages of spectra of the transmembrane potential $V$ at all spatial grid points and from all simulation runs. The spectrum of the (LR) model is characterized by a narrow peak at 3 Hz and two local maxima at about double and half of this frequency (dotted lines). A similar characterization fails for both the (TT) and the (FK) model, where the bulk of the power density is beyond such peaks. Furthermore, the full widths at half maximum (FWHM) of the displayed Gaussian peaks are given by $\delta f \approx 0.25$ Hz (central peak), $\delta f \approx 0.45$ Hz, and $\delta f \approx 2.3$ Hz for the (LR), (TT), and (FK) model, respectively.

more effective than mono-phasic (10 ms forward) pulses, see fig. 4. This is in line with earlier findings[39]. On the other hand, the defibrillation success is almost unaffected by the boundary conditions. We also estimated both the minimum electric field strength $E_{90}^{\mathrm{mono}}$ of a single monophasic pulse and $E_{90}^{\mathrm{bi}}$ of a single biphasic pulse

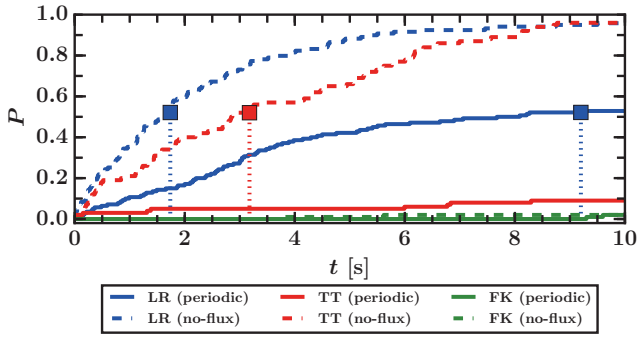


FIG. 3. (Color online) Lifetimes of electrical turbulence in the absence of defibrillation. Termination probabilities $P$ for the (LR, blue), (TT, red), and (FK, green) model with periodic (solid lines) and no-flux boundaries (dashed lines) are shown as functions of time $t$. Dotted vertical lines indicate the half-lifes $t_{1/2}$ of transient electrical turbulence.

which give rise to termination probability of at least 90%. We found $E_{90}^{\mathrm{mono}} \approx 12.6\,\mathrm{V/cm}$ and $E_{90}^{\mathrm{bi}} \approx 5.0\,\mathrm{V/cm}$ for the (LR) model, $E_{90}^{\mathrm{mono}} \approx 6.7\,\mathrm{V/cm}$ and $E_{90}^{\mathrm{S}} \approx 4.9\,\mathrm{V/cm}$ for the (TT) model, and $E_{90}^{\mathrm{mono}} \approx 20.9\,\mathrm{V/cm}$ and $E_{90}^{\mathrm{bi}} \approx 18.4\,\mathrm{V/cm}$ for the (FK) model. Systematic experiments with mono-phasic pulses applied to over 200 fibrillation episodes of canine hearts *in vivo* are consistent with our results for the (LR) and (TT) models: While defibrillation is hopeless for field strengths below 2.9 V/cm and guaranteed for field strengths above 8.5 V/cm, the regime in-between is characterized by an increasing success probability[47].

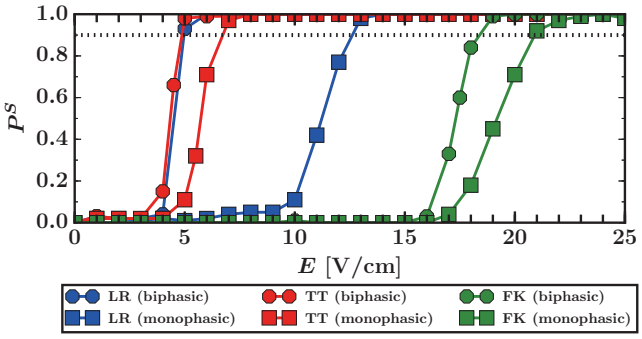


FIG. 4. (Color online) Single pulse termination probabilities $P^{\mathrm{S}}$ as functions of the applied field strength $E$ for the (LR, blue), (TT, red), and (FK, green) model, respectively, and for monophasic (squares) and biphasic (circles) pulse shapes with 10 ms duration. Shown are results of simulations with periodic boundaries, but no-flux boundaries produce an almost identical outcomes. The dotted horizontal line indicates a termination probability of 90% and defines $E_{90}$, i.e., the minimum electric field strength to obtain a termination probability of at least 90%.

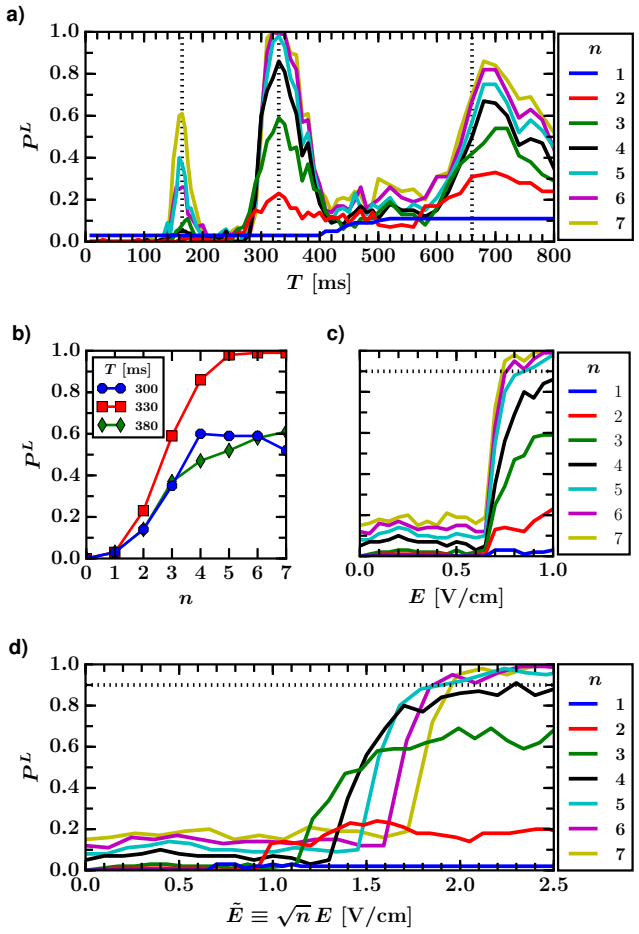


FIG. 5. (Color online) Termination probability $P^{\mathrm{L}}$ of LEAP for the (LR) model. a) $P^{\mathrm{L}}$ as a function of pulse interval $T$ for different pulse numbers $n$ and fixed field strength $E = 0.75\,\mathrm{V/cm}$. For $n \geq 3$, each curve exhibits an absolute maximum at $T_{\max} = 330\,\mathrm{ms}$ and pronounced local maxima near $T_{\max}/2$ and $2\,T_{\max}$ (vertical dotted lines). b) $P^{\mathrm{L}}$ as a function of pulse numbers $n$ for pulse intervals in the vicinity of $T_{\max} = 330\,\mathrm{ms}$ and fixed $E = 0.75\,\mathrm{V/cm}$. For $T \geq T_{\max}$, $P^{\mathrm{L}}$ monotonically increases with $n$, while for $T = 300\,\mathrm{ms}$, $n = 4$ is optimal. c) $P^{\mathrm{L}}$ as a function of $E$ for different $n$ and fixed $T = 330\,\mathrm{ms}$. LEAP becomes operative at $E$ about $0.7\,\mathrm{V/cm}$. d) $P^{\mathrm{L}}$ as a function of the rescaled field strength $\tilde{E} \equiv \sqrt{n}\,E$. The lines for $n = 5$ and $n = 6$ first exceed 90% termination probability, so we identify the optimal LEAP protocol to consist of 5 or 6 pulses.

### C. Low-energy antifibrillation pacing (LEAP)

LEAP has been defined by the reduction of the energy per pulse of several weak pulses in comparison to a single pulse[13]. Here, we adapt a stricter definition for successful LEAP by comparing the total energy of the weak pulses to the single pulse. Since single biphasic pulses are favorable for defibrillation compared to single monophasic pulses, see section III B, we employed the former for LEAP. However, we also noted that for the small field strength employed for LEAP, there is virtually no difference between the efficiencies of mono- and biphasic pulses. The overall energy delivered by a LEAP protocol is proportional to the number $n$ of pulses and the square of the electric field strength $E$. Therefore, we define the rescaled field strength $\tilde{E} \equiv \sqrt{n}\,E$ and consider LEAP with $n$ pulses to be functional if $\tilde{E}^{\mathrm{L}}_{90} < E^{\mathrm{bi}}_{90}$, where $\tilde{E}^{\mathrm{L}}_{90}$ is the rescaled electric field strength of LEAP to achieve a termination probability of 90% and $E^{\mathrm{bi}}_{90}$ is the corresponding quantity for a single biphasic pulse.

It turns out that LEAP is successful to control electrical turbulence in cardiac tissue described by the (LR) model, see fig. 5 and movies as supplementary material. However, cardiac tissue described by means of the (TT) or the (FK) model does not show an improvement for LEAP in the form of a significant total energy reduction when compared to the single shock defibrillation: For pulse intervals $T$ between 0 ms and 500 ms, pulse numbers up to $n = 10$, and rescaled field strengths up to the respective single pulse limits, LEAP is not successful for these models. For the (LR) model, the pulse interval $T$ turns out to be crucial for LEAP success, see fig. 5a. Maximal termination probability $P^{\mathrm{L}}$ is found for $T_{\max} \approx 330\,\mathrm{ms}$ which matches the dominant period $\tau \approx 330\,\mathrm{ms}$ of the fibrillation state of the (LR) model, see fig. 2. Furthermore, pulse intervals with $T_{\max}/2$ and $2\,T_{\max}$ may also be chosen for LEAP albeit they result in a smaller success probability.

Naturally, the termination probability increases with the number of pulse, except for intervals $T$ slightly below $T_{\max}$, where $n = 4$ is optimal, see fig. 5b. In this regime, the later pulses seem to reinitiate fibrillation after successful termination. Choosing the optimal interval $T_{\max}$, the minimal field strengths for a LEAP success probability of 90% are $E^{\mathrm{L}}_{90} \approx 0.85\,\mathrm{V/cm}$ and $E^{\mathrm{L}}_{90} \approx 0.76\,\mathrm{V/cm}$ for five and six pulses, respectively, see fig. 5c. In both cases, this corresponds to a rescaled field strength of $\tilde{E}^{\mathrm{L}}_{90} \approx 1.9\,\mathrm{V/cm}$, see 5d. For comparison, the field strength required for a single defibrillation pulse is $E^{\mathrm{bi}}_{90} \approx 5.0\,\mathrm{V/cm}$, i.e., the achieved total reduction of dissipated energy is about 86%, while the reduction per pulse is about 97% for five pulses and about 98% for six pulses.

For the optimal pulse interval $T_{\max}$, the termination probability $P^{\mathrm{L}}$ decreases for electric field strengths above 2.8 V/cm, see fig. 6a. In this regime, the later pulses reinitiate fibrillation after successful termination, similar to the situation depicted by the blue line in fig. 5b. In fact, the optimal pacing period does not match $T_{\max}$ which is given by the dominant period of the electrical turbulence in absence of pacing, but is shifted to about 365 ms for $E = 3\,\mathrm{V/cm}$, see fig. 6b. With this pacing period, which corresponds to 10% underdrive pacing, $E^{\mathrm{L}}_{90}$ is increased significantly to about $2.2\,\mathrm{V/cm}$ for six pulses, see fig. 6c, and the energy reduction is only 80% per pulse, resulting in no reduction of the total energy.

Our results are summarized in table I. Electrical turbulence, i.e. fibrillation, exhibits a frequency spectrum

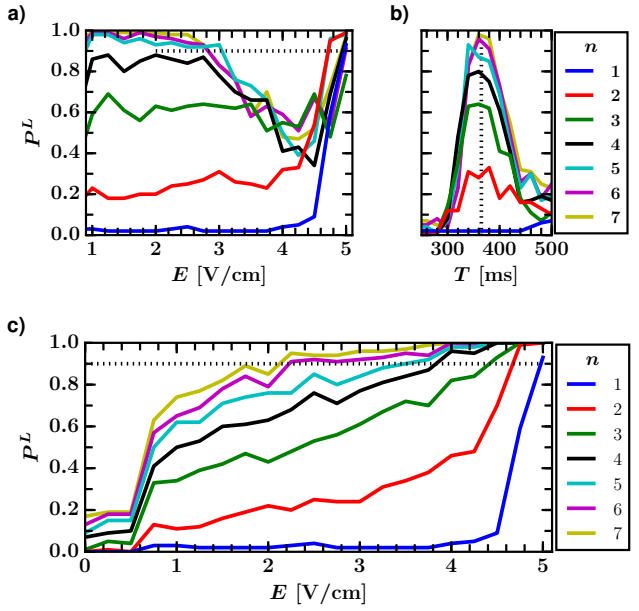


FIG. 6. (Color online) Termination probability $P^{\mathrm{L}}$ of a suboptimal version of LEAP. a) $P^{\mathrm{L}}$ as a function of (a relatively high) electric field strength $E$ for different pulse numbers $n$ and fixed $T = 330\,\mathrm{ms}$. The termination probability decreases for $E \geq 2.8$ V/cm as in this regime, the later pulses reinitiate fibrillation after successful termination. b) $P^{\mathrm{L}}$ as a function of pulse interval $T$ for different $n$ and fixed $E = 3\,\mathrm{V/cm}$. The vertical dotted line indicates the maximum at $T = 365\,\mathrm{ms}$. c) $P^{\mathrm{L}}$ as a function of $E$ for different $n$ and fixed $T = 365\,\mathrm{ms}$.

| | Electr. turbulence | | Single pulse defib. | | LEAP |
|---|---|---|---|---|---|
| | $\delta f/f$ | $t_{1/2}$ [s] | $E_{90}^{\mathrm{mono}}$ | $E_{90}^{\mathrm{bi}}$ [V/cm] | $\tilde{E}_{90}^{\mathrm{L}}$ [V/cm] |
| LR | 0.08 | 9.2 (periodic)<br>1.7 (no-flux) | 12.6 | 5.0 | 1.9<br>(5 or 6 pulses) |
| TT | 0.12 | $> 10.0$ (per)<br>3.1 (no-fl) | 6.7 | 4.9 | no |
| FK | 0.19 | $\gg 10.0$ (per)<br>$\gg 10.0$ (no-fl) | 20.9 | 18.4 | no |

TABLE I. Summary of electrical turbulence, single pulse defibrillation, and low-energy antifibrillation pacing (LEAP) probed with different cellular models. The regularity of electrical turbulence is quantified by the relative width $\delta f/f$ of the main spectral peak, see fig. 2, while its persistence with periodic and no-flux boundaries is measured by the half-life $t_{1/2}$, see fig. 3. $E_{90}^{\mathrm{mono}}$ and $E_{90}^{\mathrm{bi}}$ denote the minimal field strength of a single mono- and biphasic pulse, respectively, to achieve a 90% termination probability. Similarly, $\tilde{E}_{90}^{\mathrm{L}} \equiv \sqrt{n}\, E_{90}^{\mathrm{L}}$ is the rescaled minimal field strength for LEAP, see fig. 5d. LEAP is defined to be successful if $\tilde{E}_{90}^{\mathrm{L}} < E_{90}^{\mathrm{bi}}$ which is the case for the (LR), but not for the (TT) and (FK) model. In particular, five and six pulses spaced by the optimal pulse interval $T_{\max}$ result in $\tilde{E}_{90}^{\mathrm{L}} \approx 1.9\,\mathrm{V/cm}$ which corresponds to an energy reduction of about 86%.

with a distinct peak. For the (LR) model, this peak is relatively narrow compared to the (TT) and (FK) models. Furthermore, the (LR) spectrum exhibits peaks at about half and double of the dominant frequency, while both the (TT) and (FK) models have rather unstructured spectra. Naturally, fibrillation exhibits less persistence for no-flux boundary conditions. Furthermore, for given boundary conditions and simulation domains, electrical turbulence exhibits different persistencies in different models. However, for all models and periodic boundaries, the half-life $t_{1/2}$ of fibrillation is at least 9 s which is longer than the duration of a defibrillation protocol. LEAP does only operate in simulations with the (LR) model. Maximal reduction of the total energy of a pulse train is found for five or six pulses and a pulse interval of 330 ms.

## IV. DISCUSSION

We have performed extensive simulations of electrical turbulence, standard single pulse defibrillation, and LEAP. For each set of parameters, simulations were repeated with 100 initial conditions for the electrically turbulent state in order to determine the probability of wave termination. Heterogeneities obeying a size distribution typical for blood vessels in cardiac tissue where added and acted as virtual electrodes, i. e. centers for localized tissue activations during defibrillation. Extensive simulations were performed for three different cellular models, namely the Luo-Rudy (LR) model[32], the Ten Tusscher (TT) model[33], and a variant of the Fenton-Karma (FK) model[34] which all show somewhat different phenomenologies of spatiotemporal chaos. We found that LEAP is only successful for the (LR) model which exhibits a clear dominant period during fibrillation not present in the (TT) or the (FK) model.

The half-life of the fibrillation state depends on the cellular model, the boundary conditions, and the domain size. In order to test LEAP, we have chosen a sufficiently large domain size of 20 cm x 20 cm for all models to ensure enough persistence of turbulence. Alternatively, arrhythmias may be sustained by decreasing the tissue conductivities[29] (In this study over-driving VF with 88% of the dominant cycle length in an anatomically realistic model may result in an energy reduction of 99.5% in some simulations[29]). The relatively small half-lives of fibrillation did not seem to have misguided us in terms of LEAP success: Electrical turbulence in the (LR) model with periodic boundary conditions exhibits a half-life of about 9 seconds and can be successfully terminated by LEAP. On the other hand, turbulence in the (TT) model with no-flux boundary conditions exhibits only about 3 seconds while LEAP does not succeed in this case.

Parameters like the electric field strength, the number of pulses and the pacing period, i. e., the time between two pulses, were varied in order to determine the most efficient protocol in terms of energy reduction. It turns out that the pacing period for which LEAP works most efficiently is roughly the dominant period of the electrical turbulence. Protocols with multiples and divisors of this

optimal period have relatively high success rates too, indicating that the defibrillation process can be understood as a synchronization process. A LEAP protocol, employing resonant pacing with the mentioned dominant period and five pulses, required about 97% less energy per pulse and 86% less total energy than a single biphasic shock for successful defibrillation.

This optimal pacing is somewhat different from the over- and underdrive pacing applied in LEAP experiments[13]. For a field strength of $E = 0.75\,\mathrm{V/cm}$, employing a pulse interval of 90% or 110% of the dominant cycle length reduces the success probability to about 50% in our simulations, see fig. 5a. For larger electric field strengths, however, the optimal pacing period is slightly increased. With $E = 3\,\mathrm{V/cm}$, the optimal pacing period is at about 110% of the dominant period of electrical turbulence, see fig. 6b. This effect can be interpreted as an increased dominant period of the perturbed system: Tissue which gets excited by strong electrical fields has an increased refractory period. Underpacing with a pulse interval of $T = 365\,\mathrm{ms}$ results in an energy reduction of about 80% per pulse, see fig. 6c, but no total energy reduction. We might speculate that the experimental finding[13] of an energy reduction between 80 and 90% per pulse and successful underdrive pacing might correspond to a similar variant of LEAP.

## V. CONCLUSION

We have drawn statistically sound statements for a simple model of cardiac tissue perforated by blood vessels. We demonstrated that LEAP is only successful if the cellular model exhibits a clear dominant period during fibrillation. In this case, the pulses are most efficient with respect to defibrillation if the period between these pulses matches the dominant period of fibrillation. Using a defibrillation protocol with this period required 97 – 98% less energy per pulse, i.e. 86% less total energy than a comparable single biphasic shock for successful defibrillation. We also investigated a less efficient version of LEAP in which underdrive pacing is superior to resonant pacing. The speculation that a similar mechanism was at work in previous LEAP experiments is worth testing in future experiments.

## SUPPLEMENTARY MATERIAL

Movies of the simulations are provided online as **supplementary material**. In all movies, the simulation domain has an edge length of 20 cm and periodic boundary conditions. In movies 4 – 6, the (first) pulse is applied at $t = 500\,\mathrm{ms}$. All biphasic pulses are applied for 7 ms in forward and 3 ms in backward direction.
Movie 1: Electrical turbulence for the (LR) model.
Movie 2: Electrical turbulence for the (TT) model.
Movie 3: Electrical turbulence for the (FK) model.
Movie 4: Defibrillation with a single biphasic pulse for the (LR) model. The field strength is $E = 5\,\mathrm{V/cm}$.
Movie 5: Defibrillation with a single biphasic pulse for the (TT) model. The field strength is $E = 5\,\mathrm{V/cm}$.
Movie 6: LEAP with five biphasic pulses for the (LR) model. The field strength is $E = 0.75\,\mathrm{V/cm}$ and the pulse interval is optimal, i.e. $T = 330\,\mathrm{ms}$.

## ACKNOWLEDGMENTS

We acknowledge financial support by DFG through SFB910 (MB, SA, TN) and through GRK1558 (PB, MB). We thank Rodrigo Weber dos Santos, Flavio Fenton, Ulrich Parlitz, and Valentin Krinsky for discussions.

## REFERENCES

[1] E. M. Cherry, F. H. Fenton, and R. F. Gilmour, "Mechanisms of ventricular arrhythmias: a dynamical systems-based perspective," American Journal of Physiology-Heart and Circulatory Physiology **302**, H2451–H2463 (2012).
[2] S. V. Pandit and J. Jalife, "Rotors and the dynamics of cardiac fibrillation," Circulation research **112**, 849–862 (2013).
[3] A. Karma, "Physics of cardiac arrhythmogenesis," Annu. Rev. Condens. Matter Phys. **4**, 313–337 (2013).
[4] Z. Qu, G. Hu, A. Garfinkel, and J. N. Weiss, "Nonlinear and stochastic dynamics in the heart," Physics reports **543**, 61–162 (2014).
[5] S. Alonso, M. Bär, and B. Echebarria, "Nonlinear physics of electrical wave propagation in the heart: a review," Reports on Progress in Physics **79**, 096601 (2016).
[6] R. A. Gray, A. M. Pertsov, and J. Jalife, "Spatial and temporal organization during cardiac fibrillation," Nature **392**, 75–78 (1998).
[7] F. X. Witkowski, L. J. Leon, P. A. Penkoske, W. R. Giles, M. L. Spano, W. L. Ditto, and A. T. Winfree, "Spatiotemporal evolution of ventricular fibrillation," Nature **392**, 78–82 (1998).
[8] M. P. Nash, A. Mourad, R. H. Clayton, P. M. Sutton, C. P. Bradley, M. Hayward, D. J. Paterson, and P. Taggart, "Evidence for multiple mechanisms in human ventricular fibrillation," Circulation **114**, 536–542 (2006).
[9] K. H. Ten Tusscher and A. V. Panfilov, "Organization of ventricular fibrillation in the human heart," Circulation Research **100**, e87–e101 (2007).
[10] W. H. Maisel, "Pacemaker and icd generator reliability: meta-analysis of device registries," Jama **295**, 1929–1934 (2006).
[11] G. P. Walcott, C. R. Killingsworth, and R. E. Ideker, "Do clinically relevant transthoracic defibrillation energies cause myocardial damage and dysfunction?" Resuscitation **59**, 59–70 (2003).
[12] F. H. Fenton, S. Luther, E. M. Cherry, N. F. Otani, V. Krinsky, A. Pumir, E. Bodenschatz, and R. F. Gilmour, "Termination of atrial fibrillation using pulsed low-energy far-field stimulation," Circulation **120**, 467–476 (2009).
[13] S. Luther, F. H. Fenton, B. G. Kornreich, A. Squires, P. Bittihn, D. Hornung, M. Zabel, J. Flanders, A. Gladuli, L. Campoy, E. M. Cherry, G. Luther, G. Hasenfuss, V. I. Krinsky, A. Pumir, R. F. G. Jr, and E. Bodenschatz, "Low-energy control of electrical turbulence in the heart," Nature **475**, 235 – 239 (2011).
[14] W. Li, C. M. Ripplinger, Q. Lou, and I. R. Efimov, "Multiple monophasic shocks improve electrotherapy of ventricular tachycardia in a rabbit model of chronic infarction," Heart Rhythm **6**, 1020–1027 (2009).

[15]C. M. Ambrosi, C. M. Ripplinger, I. R. Efimov, and V. V. Fedorov, "Termination of sustained atrial flutter and fibrillation using low-voltage multiple-shock therapy," Heart Rhythm **8**, 101–108 (2011).

[16]W. Li, A. H. Janardhan, V. V. Fedorov, Q. Sha, R. B. Schuessler, and I. R. Efimov, "Low-energy multistage atrial defibrillation therapy terminates atrial fibrillation with less energy than a single shockclinical perspective," Circulation: Arrhythmia and Electrophysiology **4**, 917–925 (2011).

[17]A. H. Janardhan, W. Li, V. V. Fedorov, M. Yeung, M. J. Wallendorf, R. B. Schuessler, and I. R. Efimov, "A novel low-energy electrotherapy that terminates ventricular tachycardia with lower energy than a biphasic shock when antitachycardia pacing fails," Journal of the American College of Cardiology **60**, 2393–2398 (2012).

[18]S. Weidmann, "Effect of current flow on the membrane potential of cardiac muscle," The Journal of Physiology **115**, 227 – 236 (1951).

[19]J. P. Wikswo Jr, S.-F. Lin, and R. A. Abbas, "Virtual electrodes in cardiac tissue: a common mechanism for anodal and cathodal stimulation." Biophysical Journal **69**, 2195 (1995).

[20]A. Pumir and V. Krinsky, "Unpinning of a rotating wave in cardiac muscle by an electric field," Journal of theoretical biology **199**, 311–319 (1999).

[21]A. Pumir, V. Nikolski, M. Hörning, A. Isomura, K. Agladze, K. Yoshikawa, R. Gilmour, E. Bodenschatz, and V. Krinsky, "Wave emission from heterogeneities opens a way to controlling chaos in the heart," Physical review letters **99**, 208101 (2007).

[22]P. Bittihn, M. Hörning, and S. Luther, "Negative curvature boundaries as wave emitting sites for the control of biological excitable media," Physical review letters **109**, 118106 (2012).

[23]B. J. Caldwell, M. L. Trew, and A. M. Pertsov, "Cardiac response to low energy field pacing challenges the standard theory of defibrillation," Circulation: Arrhythmia and Electrophysiology , CIRCEP–114 (2015).

[24]S. Takagi, A. Pumir, D. Pazo, I. Efimov, V. Nikolski, and V. Krinsky, "Unpinning and removal of a rotating wave in cardiac muscle," Physical review letters **93**, 058101 (2004).

[25]C. M. Ripplinger, V. I. Krinsky, V. P. Nikolski, and I. R. Efimov, "Mechanisms of unpinning and termination of ventricular tachycardia," American Journal of Physiology-Heart and Circulatory Physiology **291**, H184–H192 (2006).

[26]A. Pumir, S. Sinha, S. Sridhar, M. Argentina, M. Hörning, S. Filippi, C. Cherubini, S. Luther, and V. Krinsky, "Wave-train-induced termination of weakly anchored vortices in excitable media," Physical Review E **81**, 010901 (2010).

[27]T. Shajahan, S. Berg, S. Luther, V. Krinski, and P. Bittihn, "Scanning and resetting the phase of a pinned spiral wave using periodic far field pulses," New Journal of Physics **18**, 043012 (2016).

[28]D. Hornung, V. Biktashev, N. Otani, T. Shajahan, T. Baig, S. Berg, S. Han, V. Krinsky, and S. Luther, "Mechanisms of vortices termination in the cardiac muscle," Open Science **4**, 170024 (2017).

[29]L. J. Rantner, B. M. Tice, and N. A. Trayanova, "Terminating ventricular tachyarrhythmias using far-field low-voltage stimuli: mechanisms and delivery protocols," Heart Rhythm **10**, 1209–1217 (2013).

[30]J. P. Keener and J. Sneyd, *Mathematical physiology*, Vol. 1 (Springer, 2009).

[31]M. M. Elshrif and E. M. Cherry, "A quantitative comparison of the behavior of human ventricular cardiac electrophysiology models in tissue" PloS one **9**, e84401 (2014).

[32]L. Luo and Y. Rudy, "A model of the ventricular cardiac action potential: depolarization, repolarization and their interaction," Circ. Res. **68**, 1501 – 1526 (1991).

[33]K. Ten Tusscher and A. Panfilov, "Cell model for efficient simulation of wave propagation in human ventricular tissue under normal and pathological conditions," Physics in medicine and biology **51**, 6141 (2006).

[34]F. Fenton and A. Karma, "Vortex dynamics in three-dimensional continuous myocardium with fiber rotation: filament instability and fibrillation," Chaos: An Interdisciplinary Journal of Nonlinear Science **8**, 20–47 (1998).

[35]N. F. Otani, A. Mo, S. Mannava, F. H. Fenton, E. M. Cherry, S. Luther, and R. F. Gilmour Jr, "Characterization of multiple spiral wave dynamics as a stochastic predator-prey system," Physical Review E **78**, 021913 (2008).

[36]S. Weidmann, "Electrical constants of trabecular muscle from mammalian heart," The Journal of Physiology **210**, 1041 – 1054 (1970).

[37]I. R. Efimov, M. W. Kroll, and P. Tchou, *Cardiac bioelectric therapy: mechanisms and practical implications* (Springer Science & Business Media, 2008).

[38]U. Achleitner, K. Rheinberger, B. Furtner, A. Amann, and M. Baubin, "Waveform analysis of biphasic external defibrillators," Resuscitation **50**, 61–70 (2001).

[39]J. Bragard, A. Simic, J. Elorza, R. O. Grigoriev, E. M. Cherry, R. F. Gilmour Jr, N. F. Otani, and F. H. Fenton, "Shock-induced termination of reentrant cardiac arrhythmias: Comparing monophasic and biphasic shock protocols," Chaos: An Interdisciplinary Journal of Nonlinear Science **23**, 043119 (2013).

[40]W. Hackbusch, *Elliptic Differential Equations: Theory and Numerical Treatment (Springer Series in Computational Mathematics)* (Springer, 2003).

[41]S. Rush and H. Larsen, "A practical algorithm for solving dynamic membrane equations," Nature **25**, 389 – 392 (1978).

[42]E. Isaacson and H. Keller, *Analysis of Numerical Methods*, Dover Books on Mathematics Series (Dover Publications, 1994).

[43]A. Winfree, "Evolving perspectives during 12 years of electrical turbulence," Chaos: An Interdisciplinary Journal of Nonlinear Science **8**, 1–19 (1998).

[44]A. Wacker, S. Bose, and E. Schöll, "Transient spatio-temporal chaos in a reaction-diffusion model," EPL (Europhysics Letters) **31**, 257 (1995).

[45]M. C. Strain and H. S. Greenside, "Size-dependent transition to high-dimensional chaotic dynamics in a two-dimensional excitable medium," Physical Review Letters **80**, 2306 (1998).

[46]R. Wackerbauer and K. Showalter, "Collapse of spatiotemporal chaos," Physical review letters **91**, 174103 (2003).

[47]F. X. Witkowski, P. A. Penkoske, and R. Plonsey, "Mechanism of cardiac defibrillation in open-chest dogs with unipolar dc-coupled simultaneous activation and shock potential recordings." Circulation **82**, 244–260 (1990).